CHINESE JOURNAL OF MECHANICAL ENGINEERING
Vol. 25, No. 3, 2012

DOI: 10.3901/CJME.2012.03.484, available online at www.springerlink.com; www.cjmenet.com; www.cjmenet.com.cn

Detached-eddy Simulation for Time-dependent Turbulent Cavitating Flows

HUANG Biao, WANG Guoyu*, YU Zhiyi, and SHI Shuguo

School of Mechanical Engineering, Beijing Institute of Technology, Beijing 100081, China

Received July 28, 2011; revised December 21, 2011; accepted January 5, 2012

Abstract: The Reynolds-averaged Navier-Stokes (RANS), such as the original k-ω two-equation closures, have been very popular in providing good prediction for a wide variety of flows with presently available computational resource. But for cavitating flows, the above equations noticeably over-predict turbulent production and hence effective viscosity. In this paper, the detached eddy simulation (DES) method for time-dependent turbulent cavitating flows is investigated. To assess the state-of-the-art of computational capabilities, different turbulence models including the widely used RANS model and DES model are conducted. Firstly, in order to investigate the grid dependency in computations, different grid sizes are adopted in the computation. Furthermore, the credibility of DES model is supported by the unsteady cavitating flows over a 2D hydrofoil. The results show that the DES model can effectively reduce the eddy viscosities. From the experimental validations regarding the force analysis, frequency and the unsteady cavity visualizations, more favorable agreement with experimental visualizations and measurements are obtained by DES model. DES model is better able to capture unsteady phenomena including cavity length and the resulting hydrodynamic characteristics, reproduces the time-averaged velocity quantitatively around the hydrofoil, and yields more acceptable and unsteady dynamics features. The DES model has shown to be effective in improving the overall predictive capability of unsteady cavitating flows.

Key words: cavitation, detached-eddy simulation, unsteady cavitating flows

1 Introduction

Cavitation can occur in a wide range of liquid flows, including those trough rotating machinery and nozzles and about underwater bodies[1–2]. This cavitation phenomenon is usually associated with performance decrease, blade erosion, vibrations that may lead to damage, and noise due to vapor collapse close to the solid wall. Therefore, it is utmost importance to understand the physical mechanisms in such instability. Recently, the Navier-Stokes equations-based modeling and simulation techniques have been proposed to simulate the cavitation physics. The closure models including turbulence and cavitation models play very important roles in the simulations of the flow phenomena. The transport-based cavitation model (TEM), which solves an additional transport equation for either the mass or volume fraction, is used very popularly[3–6]. Because of the unsteadiness of cavitating flow, the choices of turbulence models are really very critical for simulations. The original RANS turbulence model (such as k-ε and k-ω) noticeably over-predicts turbulent production and hence effective viscosity in stagnation flow regions, as pointed out by COUTIER-DELGOSHA, et al[7]. Large-eddy simulation (LES) is an alternative to RANS turbulence model that can simulate small-scale vortex shedding, but the computational cost of LES for practical problems, in terms of memory requirements and CPU-time, limits its uses to relatively high–Reynolds cavitating flows. JOHANSEN, et al[8], formulated a filter-based model (FBM) to avoid some of the known deficiencies of the RANS approaches and the difficulties in the application of LES. This model reduces the influence of turbulent eddy viscosity based on the local numerical resolution, essentially blending direct numerical simulation (DNS) and conventional turbulence model in a single framework.

In parallel, detached eddy simulation (DES) approaches have emerged recently as a potential compromise between RANS turbulence models and full LES. The advantage of the model is that the computation is less expensive than LES and more accurate than RANS computations, this hybrid modeling adopts the merit of a RANS model in simulating attached wall boundary layers with an alleviated near-wall grid resolution as compared with a wall-resolved LES, while taking the advantage of LES in resolving flows characterized by massive separation and vortex shedding in flow-detached regions. The "core" DES idea was employed in 1997 together with its formulation based on the S-A turbulence model[9]. Although, basically, nothing has changed since then, a more thoughtful definition of the technique is now available, not linked with any specific turbulence model. GEORGE, et al[10], applied different RANS models, DES model and LES to prediction of the

* Corresponding author. E-mail: wangguoyu@bit.edu.com
This project is supported by National Natural Science Foundation of China (Grant No.11172040)

flow over a sphere at Re=10^4, they concluded that DES predictions in flows with turbulence boundary-layer separation will be more sensitive to RANS modeling approximations in predicting boundary-layer growth and separation. STRELETS, et al[11], made an attempt to outline the reasoning behind and the emerging level of success of the DES of complex massively separated turbulent flows at high Reynolds number. SZYDLOWSKI, et al[12], used RANS and DES methods to simulate the flow around NACA0015 airfoil under static and dynamic stall. Their work was focused on the prediction of the stall condition over the airfoil geometry, and a good agreement between simulation results simulated by DES and experimental results was obtained. For cavitating flows, MICHAEL, et al[13], evaluated an enhanced turbulence modeling scheme based on DES, the results showed that a standard RANS model degraded the ability to predict marginally stable cavities whereas the DES model appeared to yield more accurate flow modeling, possibly because DES handles large scale closure dynamics better.

The present study is aimed at evaluating DES model for time-dependent cavitating flows. The unsteady cavitating flow around the Clark-Y hydrofoil at high Re number is investigated; experimental visualization and data serving as a reference will be gauged for comparisons. In addition, interesting unsteady numerical results are presented in a held form for comparison with photographic visualization, and also some intriguing results due to the nature of unsteady cavitating multiphase flow will be discussed.

2 Governing Equations and Numerical Techniques

The set of governing equations for isothermal cavitation under the homogeneous-fluid modeling consists of the conservative form of the Favre-averaged Navier-Stokes equations, and also a transport equation for the liquid volume fraction is considered as the transfer of liquid and vapor states. The continuity, momentum, and cavitation model equations are given as below:

$$\frac{\partial \rho_{\mathrm{m}}}{\partial t}+\frac{\partial(\rho_{\mathrm{m}} u_j)}{\partial x_j}=0, \tag{1}$$

$$\frac{\partial(\rho_{\mathrm{m}} u_i)}{\partial t}+\frac{\partial(\rho_{\mathrm{m}} u_i u_j)}{\partial x_j}=-\frac{\partial p}{\partial x_i}+\frac{\partial}{\partial x_j}\left[(\mu_{\mathrm{L}}+\mu_{\mathrm{T}})\left(\frac{\partial u_i}{\partial x_j}+\frac{\partial u_j}{\partial x_i}-\frac{2}{3}\frac{\partial u_k}{\partial x_k}\delta_{ij}\right)\right], \tag{2}$$

$$\frac{\partial \alpha_l}{\partial t}+\frac{\partial(\alpha_l u_j)}{\partial x_j}=\dot{m}^{+}+\dot{m}^{-}. \tag{3}$$

The mixture property ϕ_{m}, can be expressed as

$$\phi_{\mathrm{m}}=\varphi_{\mathrm{l}}\alpha_{\mathrm{l}}+\varphi_{\mathrm{v}}(1-\alpha_{\mathrm{l}}), \tag{4}$$

where x and the indices i, j and k denote the coordinate axes, t is time, ρ_{m} is the mixture density, u represents the velocity components, p is the pressure, μ denotes viscosity, α represents the volume fraction, $\dot{m}^{+}$ and $\dot{m}^{-}$ are source term sink term respectively, and the subscripts l, v, L, and T denote the liquid phase, vapor phase, laminar flow and turbulent flow, respectively. ϕ can be density, viscosity, etc.

2.1 Turbulence model

RANS solutions are obtained by solving the Reynolds-averaged and turbulence model equation in a time-accurate fashion. In present study, the k-ω based on SST model is investigated as the RANS model. The SST model accounts for the transport of the turbulent shear stress and gives highly accurate predictions of the onset and the amount of flow separation under adverse pressure gradients, the proper transport behavior can be obtained by a limiter to the formulation of eddy-viscosity; the SST model is defined in Ref. [16]:

$$\frac{D\rho k}{Dt}=P_k-\frac{\rho k^{3/2}}{l_{k-\omega}}+\frac{\partial}{\partial x_i}\left[\left(\mu+\frac{\mu_t}{\sigma_k}\right)\frac{\partial k}{\partial x_i}\right], \tag{5}$$

$$\frac{D\rho\omega}{Dt}=C_w P_w-\beta_w\rho\omega^2+\frac{\partial}{\partial x_i}\left[\left(\mu+\frac{\mu_t}{\sigma_k}\right)\frac{\partial k}{\partial x_i}\right]+2\rho(1-F_1)\sigma_{\omega 2}\frac{1}{\omega}\frac{\partial k}{\partial x_i}\frac{\partial \omega}{\partial x_i}. \tag{6}$$

All the coefficients are listed for completeness in Ref. [16], and the eddy-viscosity is defined as

$$\nu_t=\frac{a_1 k}{\max(a_1\omega;\Omega)}. \tag{7}$$

With a_1 being a constant, Ω is shear-strain rate. The length scales of the model in terms of k and ω reads

$$l_t=\frac{k^{1/2}}{\beta_k\omega}. \tag{8}$$

The idea behind the DES model for Strelets [11] is to switch from the SST-RANS model to a LES model in regions where the turbulent length, predicted by the RANS model is larger than the local grid spacing. In this case, the length scale used in the computation of the dissipation rate in the equation for the turbulent kinetic energy is replaced by the local grid spacing Δ. Here, Δ is based on the largest dimension of the grid cell:

$$\Delta=\max(\Delta x,\Delta y,\Delta z),$$

$$\varepsilon = \beta_k k\omega = \begin{cases} \dfrac{k^{3/2}}{C_{\mathrm{DES}}\Delta}, C_{\mathrm{DES}}\Delta < l_{k-\omega}, \\ \dfrac{k^{3/2}}{l_t}, C_{\mathrm{DES}}\Delta \geqslant l_{k-\omega}. \end{cases} \tag{9}$$

In Eq. (9), C_{DES}=0.65. For wall-bounced separated flows, the above formulation results in a hybrid model that functions as the standard SST model inside the whole attached boundary layer, and as its subgrid-scale version in the near wake [11].

2.2 Transport-based cavitation model

Cavitation process is governed by mass and kinetics of the vapor and water phase change in the system. These issues are modeled with the aid of a transport equation with the source terms regulating the evaporation and condensation of the phases.

The source term $\dot{m}^+$ and sink term $\dot{m}^-$ in Eq. (3) represent the condensation and evaporation rates. In the present study, a popular phenomenological model originally proposed by KUBOTA, et al[3] is applied. In this model, the growth and collapse of a bubble cluster are given by a modified Rayleigh-Plesset equation, which provides the rate equation controlling vapor generation and condensation. The Rayleigh-Plesset equation is given as

$$R_{\mathrm{B}} \frac{\mathrm{d}^2 R_{\mathrm{B}}}{\mathrm{d}t^2} + \frac{3}{2}\left(\frac{\mathrm{d}R_{\mathrm{B}}}{\mathrm{d}t}\right)^2 + \frac{2\sigma}{R_{\mathrm{B}}} = \frac{p_{\mathrm{v}} - p_{\infty}}{\rho_{\mathrm{l}}}, \tag{10}$$

where ρ_{l} is the liquid density, R_{B} represents the bubble diameter, p_{v} is the pressure in the bubble (assumed to be the vapor pressure in the local temperature), p_{∞} is the reference pressure and σ is the surface tension coefficient between the liquid and vapor. Neglecting the second order terms and the surface tension, this equation reduces to

$$\frac{\mathrm{d}R_B}{\mathrm{d}t} = \sqrt{\frac{2}{3}\frac{p_{\mathrm{v}} - p}{\rho_{\mathrm{l}}}}. \tag{11}$$

The representative liquid-vapor evaporation and condensation rates for this category are shown as follows:

$$\begin{cases} \dot{m}^- = -C_{\mathrm{dest}} \dfrac{3\alpha_{\mathrm{v}}}{R_{\mathrm{B}}} \left(\dfrac{2}{3}\dfrac{p_{\mathrm{v}} - p}{\rho_{\mathrm{l}}}\right)^{1/2}, \\ \dot{m}^+ = C_{\mathrm{prod}} \dfrac{3\alpha_{\mathrm{v}}}{R_{\mathrm{B}}} \left(\dfrac{2}{3}\dfrac{p_{\mathrm{v}} - p}{\rho_{\mathrm{l}}}\right)^{1/2}, \end{cases} \tag{12}$$

where C_{prod} and C_{dest} are two empirical coefficients, designed to account for the fact that may occur at different rates (condensation is usually much slower than vaporation). To obtain an interphase mass transfer rate, further assumptions regarding the bubble concentration and radius are required. The Kubota cavitation model uses the following defaults for the model parameters: R_{B}=1 μm, C_{prod}=50, C_{dest}=0.01.

3 Results and Discussions

3.1 Grid sensitivity of detached eddy simulation

The computational domain and boundary conditions are given according to the experimental setup in Ref. [14], which is shown in Fig. 1. The Clark-Y hydrofoil is placed in the center of water tunnel with angle of attack equals to 8º. The Reynolds number and the cavitation number are 7×10^5 and 0.8, respectively, and the flow is basically turbulent with cavity shedding under the current flow conditions.

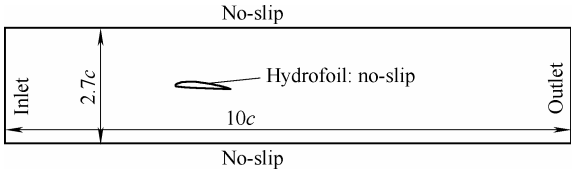

Fig. 1. Boundary conditions for Clark-Y hydrofoil

To investigate the effect of grid resolution on numerical accuracy, the sensitivity, we use three different levels of grids: coarse grid, baseline grid and fine grid listed in Table 1 and Table 2. The computational domains with 16 000, 22 000, 40 000, and 62 000 cells are applied respectively. The influence of the grid size on the results with the filter-based viscosity model is tested in Table 1. We obtain less deviation between the coarse grid and the baseline one and this difference is less than 6% between the reference and the finest one.

Table 1. Different grid conditions and corresponding behaviors with RANS model

Grid size	Frequency f/Hz	Lift coefficient C_{l}	Drag coefficient C_{d}
Coarse1 16 000	21.0	0.690	0.105
Coarse2 22 000	21.3	0.695	0.108
Baseline 40 000	21.8	0.706	0.112
Fine 62 000	21.9	0.708	0.114
Experimental data in Refs. [14–15]	24.1	0.760	0.119

Table 2. Different grid conditions and corresponding behaviors with DES model

Grid size	Frequency f/Hz	Lift coefficient C_{l}	Drag coefficient C_{d}
Coarse1 16 000	21.4	0.692	0.106
Coarse2 22 000	21.7	0.669	0.116
Baseline 40 000	24.4	0.694	0.117
Fine 62 000	24.3	0.695	0.120
Experimental data in Refs. [14–15]	24.1	0.760	0.119

Furthermore, the time-averaged drag coefficient, lift coefficient, and the frequency obtained by DES simulations are also provided to compare with experimental data in

Table 2. Fig. 2 shows the time-averaged flow structures and liquid volume fractions got by different grid size. It is clear that the cavitation structures consist of two parts, which are attached and detached cavity respectively. The attached cavity is located in the leading edge of the hydrofoil, while the detached cavity is formed due to the re-entrant jet and overlaps with the recirculation zone near the trailing edge. For the coarse grid conditions of 16 000 cells and 22 000 cells in Figs. 2(a) and 2(b), the visualizations of time-averaged cavity are very similar, and the only difference is that the size of the detached cavity is slightly larger for the 22 000 total cells. For the baseline and fine grid size in Figs. 2(c) and 2(d), a bigger time-averaged cavity size is obtained. This is due to the faster frequency than by the other grid conditions among all the cases in Table 2.

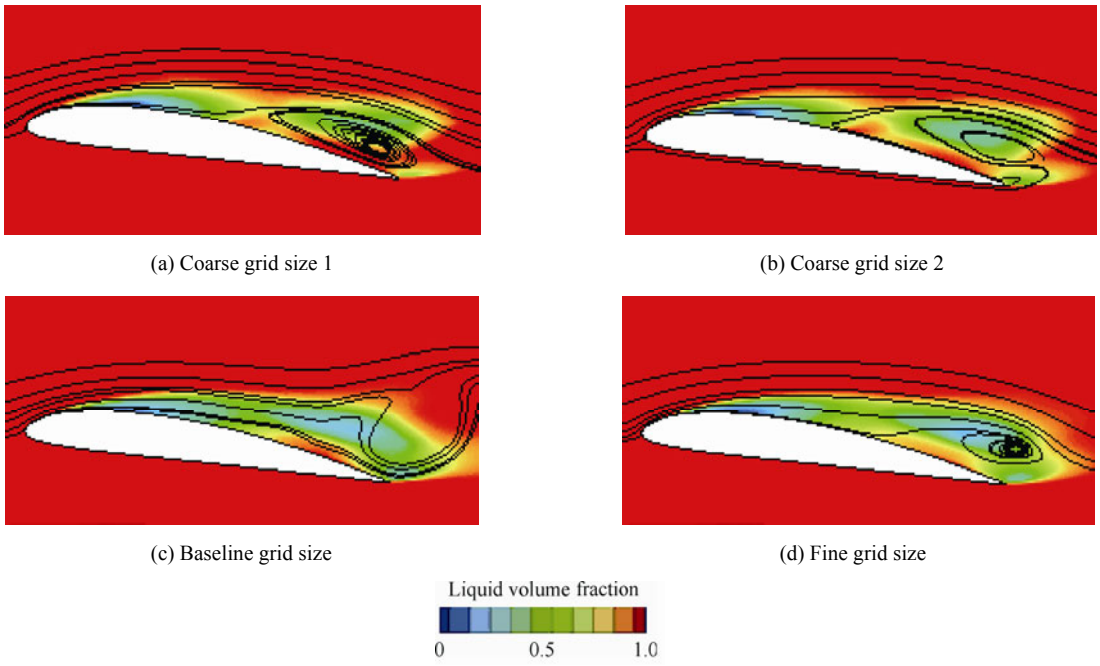

(a) Coarse grid size 1 (b) Coarse grid size 2

(c) Baseline grid size (d) Fine grid size

Fig. 2. Time-averaged liquid volume fraction contour and representative streamlines

3.2 Applications of DES model for unsteady cavitating flow

In this section, the capability of the different turbulence models is further investigated in unsteady cavitating flows over a Clark-Y hydrofoil, assessed by experimental data from WANG, et al[14]. In order to compare the two models well, the RANS model and DES model are carried out on the identical grids—baseline grid which has mentioned above. There are two model combinations listed in Table 3, the time-averaged drag, lift coefficient, and the frequency obtained by numerical simulations are also provided to compare with experimental data.

Table 3. Model combinations and corresponding behaviors

Model combinations	Cavitation model	Turbulence model	Frequency f/Hz	Lift coefficient C_l	Drag coefficient C_d
Kubota model-RANS	Kubota model	RANS	21.4	0.706	0.112
Kubota model-DES	Kubota model	DES	24.4	0.694	0.117
Experimental data in Refs. [14–15]			24.1	0.760	0.119

3.2.1 Unsteady cavity visualization and flow structure

The instantaneous contours of liquid volume fraction are compared with experimental data side by side in Fig. 3, although the frequencies are different between the CFD results and experimental data, the cavity visualizations are placed according to 20%, 50%, 70% and 90% of each corresponding cycle. For RANS model in Fig. 3, the density inside the detached cavity still contains 50% of liquid phase during 50% to 70% cycle. The higher eddy viscosity of RANS near the closure region will dissipate the detached cavity faster than that of DES. As the results, the RANS model can't capture the detached cavity during 90% of the cycle. As for the attached cavity, the maximum cavity length is no more than 50%c, where c is the chordwise of the hydrofoil.

As for the DES model, the features of every stage in experiment can be well-captured, including the detached cavity in the trailing edge of the last stage, and it will disappear before 120%c, which is more consistent to the observation experimentally. For the attached cavity, the maximum cavity can reach slightly more than 80%C, which is more substantial than that of RANS model. The density is still high during 50% of the cycle before it is fully detached. DES model weakens the dissipation so that the detached cavity is well-captured in the last stage.

Overall, there is a good agreement between the numerical and experimental results. The external shape and

global structure of both attached cavity and vapor cloud shedding are achieved. The large-scale shedding on the rear part of the sheet cavity predicted DES model are more obvious than the RANS model.

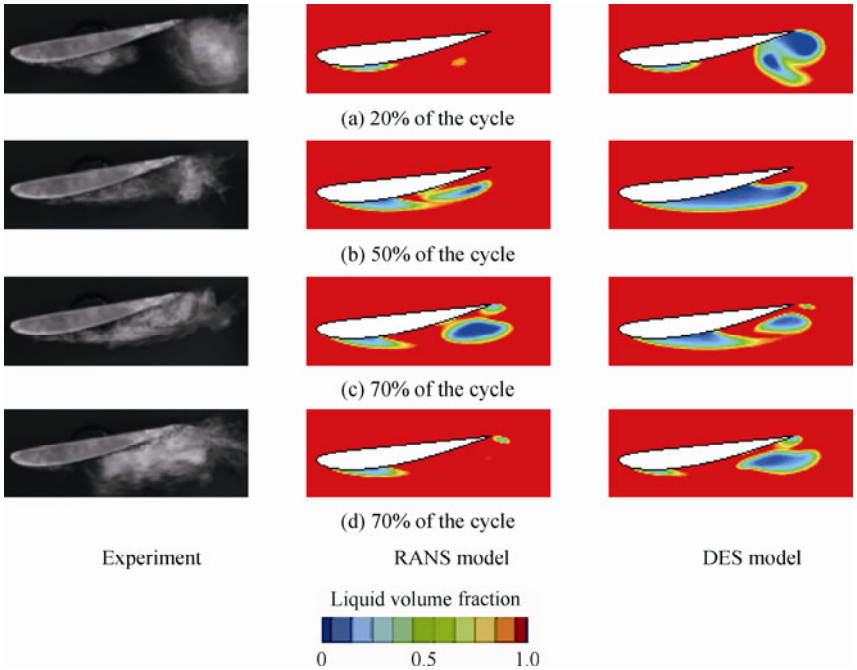

Fig. 3.　Instantaneous contours of liquid volume fraction

As mentioned above, different cavity shapes, especially in the closure region predicted by the different turbulence models, implying that the eddy viscosity distributions are handled differently. For the 2D Clark-Y hydrofoil, the cavity obtained by the RANS model turns to a stable attached sheet with the length much shorter than the experimental ones. To explain these reasons, we further compare the time-averaged eddy viscosity distributions yielded by the both turbulence models with the same cavitation number ($\sigma = 0.8$) at angle of attack (AoA) is 8°. It can be seen in Fig. 4 where an unrealistically high eddy viscosity region is developed over nearly the entire suction side surface for RANS model, resulting in reduced unsteadiness of the computed flow field.

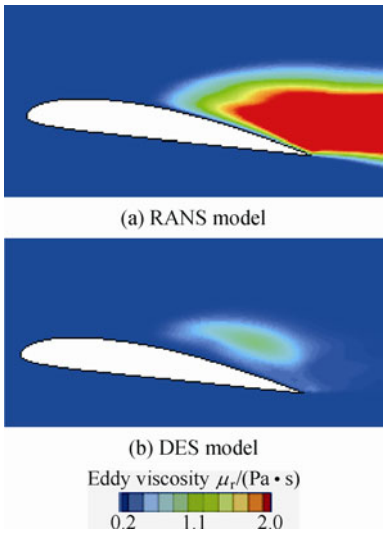

Fig. 4.　Time-averaged eddy viscosity contours with different turbulence models

The qualitative differences in the time averaged viscosity distributions between RANS and DES calculations are a consequence of the large eddies being resolved in DES and the SGS viscosity levels in these turbulence regions are higher than in the surrounding flow. In RANS model, the distribution of eddy viscosity reflects the time-averaged values in the wake where the shedding is not well represented; while the DES results show the correlation with the shed structures in the wake.

3.2.2　Time-averaged velocity profiles

The time-averaged x-direction velocity of the flow field is illustrated in Fig. 5. These time-averaged velocity profiles are tracked along the vertical direction at different locations, namely, x/c=20%, 40%, 60%, 80%, 100%, and 120%. Here, x is the coordinate axe and c denotes the chord length of the hydrofoil. The difference between CFD results and experimental data becomes more substantial, especially after the closure region. All in all, the agreement is reasonable if we consider the difficulties in experimental measurement[13]. As can be seen that even the time-averaged velocity profiles are very consistent for each model combination, however, in the chordwise location of 120%c, the difference of velocity distribution seems noticeable, the introduction of DES model led to an effective viscosity that depends on both turbulence quantities and the filter size itself. The solution on DES model is in a good agreement with experimental data, demonstrating that the DES model can produce better resolutions to simulate the fluid physical behaviors at the scales where numerical resolutions are satisfactory.

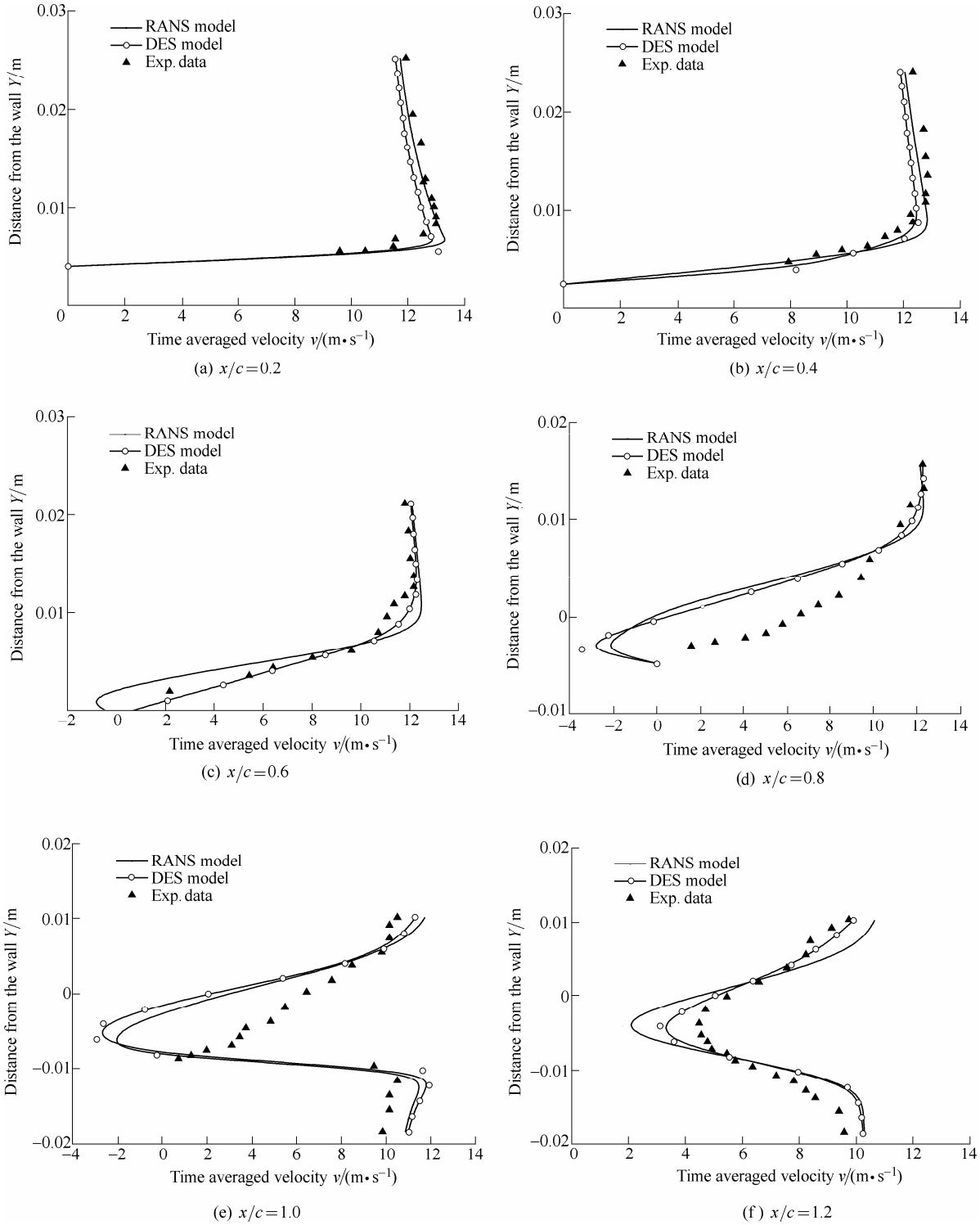

Fig. 5. Time-averaged x-direction velocity at different locations

3.2.3 Lift and drag coefficient

The corresponding lift coefficient variations for unsteady cavitating case compared with the experimental data are presented in Fig. 6. First of all, both the lift signals are seen to exhibit periodic behaviors within the time-span during which the force signals were processed. But the lift signals from the DES predictions look quite similar in that they show an identifiable periodicity, that the lift force signals are well corrected, and that large peaks are seen to occur. This is because the DES successfully predicts the vapor cloud shedding, causing the lift increases very rapidly while the cloud cavity collapse and the sheet cavity starts filling the rest of the suction side. From the instantaneous flow structures in Fig. 3, the cavity changes the effective shape of the hydrofoil more substantially, which causes the flow separates more easily with faster frequencies in Table 3. Therefore, the smaller mean lift force for DES model is expected.

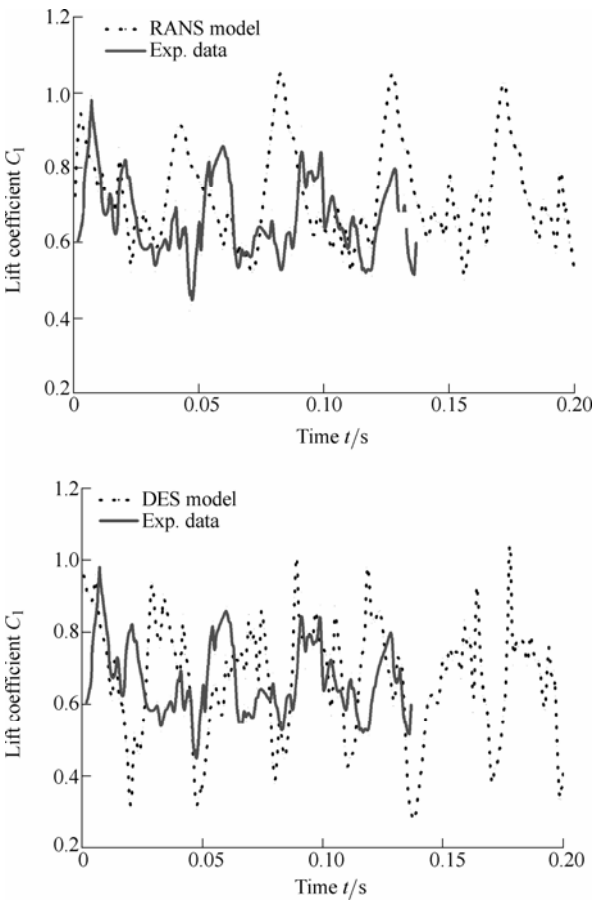

Fig. 6. History profile of lift coefficient

4 Conclusions

(1) Both coarse and fine girds reproduce the time averaged experimental results quantitatively. However, by refining the grid we see effective eddy-viscosity reduction near the closure regions, which results in slightly bigger detached cavity within a lower density inside due to the weaker dissipation of eddy viscosity in this area.

(2) On the same relative fine grid size, the more favorable agreement with experimental visualizations and measurements are obtained by DES: The cavity shapes and lengths predicted by DES are better consistence with experimental visualizations comparing with the RANS model, and also, DES model leads to the formation and shedding of large-scale vortex flows, resulting in unsteady cavitation.

(3) Because DES handles the large scale closure better than RANS models, the numerical results with DES model reproduce the time averaged velocity results quantitatively around the hydrofoil compared with the RANS models. In comparison to the RANS models, DES model yield more acceptable and unsteady dynamics features and it is a more comprehensive validation of the techniques for unsteady cavitating flows.

References

[1] KNAPP R T, DAILY J W, HAMMITT F G. *Cavitation*[M].New York: McGraw-Hill, 1970.

[2] WANG Fujun, ZHANG Ling, LI Yaojun, et al. Some key issues of unsteady turbulence numerical simulation in axial-flow pump[J]. *Chinese Journal of Mechanical Engineering*, 2008, 44(8): 73–77.

[3] KUBOTA A, KATO H, YAMAGUCHI H. A new modeling of cavitating flows: a numerical study of unsteady cavitation on a hydrofoil section[J]. *J. Fluid Mech.*, 1992, 240: 59–96.

[4] MERKLE C L, FENG J Z, BUELOW P E O. Computational modeling of the dynamics of sheet cavitation[C/CD]//*Proc. Third International Symposium on Cavitation*, Grenoble, France, 1998.

[5] KUNZ R F, BOGER D A, STINEBRING D R A. A preconditioned Navier-Stokes method for two-phase flows with application to cavitation predition[J]. *Comput. Fluid*, 2000, 29: 849–875.

[6] SINGHAL A K, ATHAVALE M M. Mathematical basis and validation of the full cavitation model[J]. *Journal of Fluids Engineering*, 2002, 124: 617–624.

[7] COUTIER-DELGOSHA O, FORTES-PATELLA R, REBOUND J L. Evaluation of the turbulence model influence on the numerical simulations of unsteady cavition[J]. *J. Fluids Eng*., 2003, 125: 33–45.

[8] JOHANSEN S T, WU J, SHYY W. Filter-based unsteady RANS computations[J]. *Int. J.Heat and Fluid Flow*, 2004, 25(1): 10–21.

[9] SPALART P R, JOU W H, STRELETS M, et al. Comments on the feasibility of LES for wings, and on a hybrid RANS/LES approach, advances in DNS/LES[C]//*First AFOSR International Conference on DNS/LES*, Greyden, Columbus, OH, 1997, 2001: 102–114.

[10] GEORGE S. Constantinescu. LES and DES investigations of turbulent flow over a sphere[G]. *AIAA* 2000-0540.

[11] STRELETS M. Detached eddy simulation of massively separated flows[G]. *AIAA* 2001-0879.

[12] SZYDLOWSKI J, COSTES M. Simulation of flow around a NACA0015 airfoil for static and dynamics stall configurations using RANS and DES[C]//*AHS International 4th Decennial Specialists Conference on Aeromechanics*, San Francisco, CA, United States, 2004: 223–238.

[13] MICHAEL P Kunzel, JULES W Lindau, LEONARD J Peltier, et al. Detached-eddy simulations for cavitating flows[G]. *AIAA* 2007-4098.

[14] WANG G Y, SENOCAK I, SHYY W. Dynamics of attached turbulent cavitating flows[J]. *Progress in Aerospace Sciences*, 2001, 37(6): 551–581.

[15] WANG G, ZHANG B, HUANG B, et al. Unsteady dynamics of cloudy cavitating flows around a hydrofoil[C/CD]//*Proceedings of the 7th International Symposium on Cavitation*, August 17–22, 2009, Ann Arbor, Michigan, USA, CAV2009, Paper No. 9.

[16] FLORIAN R, MENTER. Zonal two equation k-ω turbulence models for aerodynamic flow[G]. *AIAA*-93-2906, 1993.

Biographical notes

HUANG Biao, born in 1985, is currently a PhD candidate at *Beijing Institute of Technology, China*. His research interests include the numerical simulation of multiphase cavitating flows. Tel: +86-13522823488; E-mail: huangbiao@bit.edu.cn

WANG Guoyu, born in 1961, is currently a professor at *Beijing Institute of Technology, China*. He received his PhD degree from *Tohoku University, Japan*, in 1999. His research interests include the fluid machinery and engineering and the mechanism of cavitation and supercavitation flow.

YU Zhiyi, born in 1975, is currently an associate professor at *Beijing Institute of Technology, China*. He received his PhD degree from *Tsinghua University, China*, in 2005. His research interests include numerical simulation of multiphase flows.

SHI Shuguo, born in 1983, is currently a PhD candidate at *Beijing Institute of Technology, China*. Her research interests include the numerical simulation of multiphase cavitating flows.